Experimental Neurology 359 (2023) 114261

Contents lists available at ScienceDirect

Experimental Neurology

journal homepage: www.elsevier.com/locate/yexnr

Research paper

Movement decoding using spatio-spectral features of cortical and subcortical local field potentials

Victoria Peterson [a,*], Timon Merk [b], Alan Bush [a], Vadim Nikulin [c], Andrea A. Kühn [b], Wolf-Julian Neumann [b,1], R. Mark Richardson [a,1]

[a] Department of Neurosurgery, Massachusetts General Hospital, Harvard Medical School, Boston, USA
[b] Movement Disorder and Neuromodulation Unit, Department of Neurology, Charité – Universitätsmedizin Berlin, Berlin, Germany
[c] Department of Neurology, Max Planck Institute for Human Cognitive and Brain Sciences, Leipzig, Germany

ARTICLE INFO

Keywords:
Adaptive deep brain stimulation
Movement decoding
Machine learning
Multichannel recordings
Invasive neural oscillation
Spatial filters

ABSTRACT

The first commercially sensing enabled deep brain stimulation (DBS) devices for the treatment of movement disorders have recently become available. In the future, such devices could leverage machine learning based brain signal decoding strategies to individualize and adapt therapy in real-time. As multi-channel recordings become available, spatial information may provide an additional advantage for informing machine learning models. To investigate this concept, we compared decoding performances from single channels vs. spatial filtering techniques using intracerebral multitarget electrophysiology in Parkinson's disease patients undergoing DBS implantation. We investigated the feasibility of spatial filtering in invasive neurophysiology and the putative utility of combined cortical ECoG and subthalamic local field potential signals for decoding grip-force, a well-defined and continuous motor readout. We found that adding spatial information to the model can improve decoding (6% gain in decoding), but the spatial patterns and additional benefit was highly individual. Beyond decoding performance results, spatial filters and patterns can be used to obtain meaningful neurophysiological information about the brain networks involved in target behavior. Our results highlight the importance of individualized approaches for brain signal decoding, for which multielectrode recordings and spatial filtering can improve precision medicine approaches for clinical brain computer interfaces.

1. Introduction

Deep brain stimulation (DBS) of the subthalamic nucleus (STN) or the globus pallidus internus (GPi) is an effective symptomatic treatment for patients with Parkinson's disease (PD) (Schuepbach et al., 2013; Deuschl et al., 2006). In order to minimize potential side-effects of continuous stimulation, closed-loop or adaptive DBS (aDBS), is being investigated to reduce the amount of unnecessary stimulation delivered to the brain (Cagnan et al., 2019). In this sense, aDBS devices are bidirectional invasive brain-computer interfaces (BCI) that can adapt stimulation according to brain signals.

The viability and success of bidirectional BCIs for aDBS strongly depends on the identification of reliable biomarkers reflecting patients' symptom severity and change with treatment, as well as on the computational strategies used for neural decoding of such states and behavior. This will allow to augment aDBS strategies with machine learning, e.g. by decoding kinematic parameters which could be used in the future to refine stimulation parameters (Neumann et al., 2019). It has been shown that behavioral neural biomarkers can be identified from local field potentials (LFPs) in the STN (Little et al., 2013; Priori et al., 2013), electrocorticography (ECoG) (Swann et al., 2018) or the combinational use of both (Ferleger et al., 2020; Gilron et al., 2021).

Despite the variety of electrode contacts used during invasive brain monitoring, most of the decoding approaches in the context of adaptive DBS are based on one or two channel recordings per target structure (Gilron et al., 2021; Opri et al., 2020). That is also the case for the novel commercially available adaptive DBS devices on the market, in which one recording channel per hemisphere is used to build the bidirectional communication (Feldmann et al., 2021). The use of multichannel decoding models that inform an aDBS strategy using the patient's electro-clinical state likely would increase treatment flexibility and effectiveness.

* Corresponding author at: Thier Building, 4th floor, Massachusetts General Hospital, 50 Blossom St., Boston, MA 02114, USA.
E-mail address: vpeterson2@mgh.harvard.edu (V. Peterson).
[1] Equal contribution.

https://doi.org/10.1016/j.expneurol.2022.114261
Received 31 January 2022; Received in revised form 26 September 2022; Accepted 25 October 2022
Available online 29 October 2022

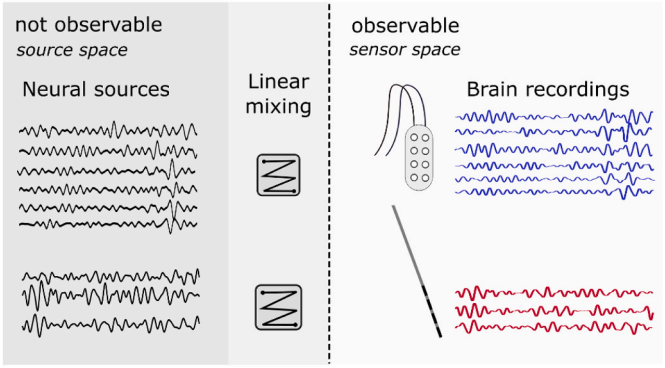

Fig. 1. Illustration of the generative statistical model in invasive neurophysiology. The true neural sources are inferred by unobservable source space signals. These sources are mixed to constitute the sensor space signals (e.g. ECoG/STN-LFP). Spatial filters aim at estimating the sources by projecting the data in the sensor space to the source space.

Due to volume conduction, the activity from a given neural population is always mixed with the activity from other populations, making inferences about the activity from a specific pool of neurons challenging (Sabbagh et al., 2020). Statistical generative models often assume that brain signals arise from activity of uncorrelated sources, and that such sources appear distorted in the signal recording as a consequence of a linear mixing (due to volume conduction), as illustrated in Fig. 1. While the spatial signal-to-source relationship is more precise in the field of invasive neurophysiology, the same underlying mechanisms are at play, and invasive recordings are contaminated by a mix of local and distant (volume conducted) brain activity (Schaworonkow and Voytek, 2021).

To effectively take advantage of multichannel neural recording, spatial filters can be used to reduce the dimensionality of the data while extracting decoding features. These source separation methods allow the computation of a new spatially filtered signal trace based on a predefined optimization criterion, in order to extract the relevant spatial information embedded in multivariate (multichannel) signals (Schaworonkow and Voytek, 2021). They directly work in the channel-time space of the signal, capturing spatial relationships of the brain recordings. In the particular case of statistical spatial filters (Fig. 1), the unobservable neural sources are estimated via decomposition of the multichannel brain recording, i.e., by demixing the observable brain signals.

Among the different spatial filtering methods that can be found in the BCI literature (Wu et al., 2018), the source power comodulation (SPoC) method (Dähne et al., 2014) is probably the most suitable approach for linking brain-power modulations to a specific target signal (i.e. kinematic parameters, reaction times, etc). Recently, it has been shown that reliable neural biomarkers related to movement in PD patients can be found via SPoC in non-invasive EEG (Castaño-Candamil et al., 2020). Until now, however, data-driven spatial filtering decoding models in invasive electrophysiology for movement decoding in PD patients have not been reported. In this study, we compared the use of a multichannel-based spatial filters approach, including analysis of the combinational use of subcortical and cortical recordings, to that of a single-channel approach. We constructed subject-specific ML-based invasive neurophysiology decoding models based on both the frequency and the spatial dimensions of the recorded brain activity, using a strategy that combines a filter-bank analysis with a spatial filtering approach. A multiple recording site (STN-LFP and ECoG) dataset from eleven (11) PD patients who performed a hand movement task during awake DBS implantation surgery was used. The task comprised both contra- and ipsilateral movements with respect to the electrode localization. A generalized linear model (GLM) with Poisson-like regularized regression was implemented for predicting the movement. We evaluated regression performance of the model in two modalities: i) single recording site, in which either ECoG or STN-LFP recordings were used as inputs to the decoding model and ii) multiple recording sites, in which both ECoG and STN-LFP recordings were used together to train the model. Since spatial filters were used, the solution was subjected to neurophysiological interpretation. We analyzed how band-power features and brain recording modalities contribute to movement decoding. We found that multichannel approaches have the potential to improve movement decoding as compared to a single-channel approach. This study advances the use of ML methods with multichannel and multiple site recordings for the potential development of intelligent aDBS devices, taking into account the spatial information of recording sites. The source code used throughout this work is available at GitHub https://github.com/Brain-Modulation-Lab/Paper_SpatialPatternsMovementDecoding

2. Materials and methods

2.1. Data

The dataset used in this study (available upon request) corresponds to that from previously published studies (Alhourani et al., 2020; Kondylis et al., 2016) and is comprised of subthalamic LFP and subdural ECoG recordings simultaneously acquired from 11 PD patients (1 female, mean age ± SD = 60.1 ± 8.3 years, disease duration ± SD = 9.8 ± 4.0 years) undergoing DBS implantation surgery. All subjects were recommended for surgery by a multidisciplinary review board and provided written informed consent. The study was approved by the Institutional Review Board of the University of Pittsburgh (IRB Protocol #PRO13110420). UPDRS Part III scores for the off-medication conditions were collected in a time period of 1–3 months prior to surgery by movement disorder neurologists. Antiparkinsonian medications were held off for at least 12 h prior to intraoperative testing.

Subjects were instructed to press a hand-grip force transducer with either their right or left hand after a visual cue appeared within a traffic light money-rewarding game. A trial begun by illuminating the yellow light in the traffic light. Patients were instructed to press the hand-grip force only when the green light (GO cue) was illuminated. If the red light (No-GO) was illuminated and the patient did press the hand-force, that trial was considered as error. The laterality of the movement (contra- or ipsilateral) was annotated with respect to the electrodes' hemisphere localization. A trial was considered successful if the subject was able to maintain for at least 100 ms with the indicated hand at least 10% of their maximum voluntary grip force. Each trial was followed by a variable inter-trial interval of 1000–2000 ms, after feedback presentation. During the task, subjects were fully awake. No anesthetic agents were administered for at least 1 h prior to the task procedure. No medication was given during the task. Only correct hand-grip force trials (GO cue) are considered for the further analysis. The number of trials performed by each patient varied between 9 and 65.

ECoG recording were acquired using 6 (7 patients), 8 (2 patients), or 28 (2 patients) contacts electrode strips (Ad-Tech, Medical Instrument Corporation), placed as close as possible to the hand knob area through the burr hole used for DBS lead implantation (Sisterson et al., 2021). Ground and reference electrodes were placed in the shoulder and mastoid, respectively. LFPs from the STN were recorded using a clinical four contacts DBS lead (model 3389, Medtronic). Data was sampled at 1000 Hz and band-pass filtered (0.3–250 Hz), using a Grapevine neural interface processor (Ripple Inc.). In order to minimize noise from cortical signals and ensure recordings were comparable to future real applications, LFP from the STN were re-referenced offline to a bipolar montage by referencing each contact to its immediate neighbor, thus three new bipolar channels were generated after this procedure.

All the analog signals, corresponding to the grip-force output, were processed offline to remove baseline drift, by estimating the baseline using the optimization problem proposed in (Xie et al., 2018) and then subtracting it from the original output. After this procedure, the grip-force output was normalized between zero (0) and one (1), where

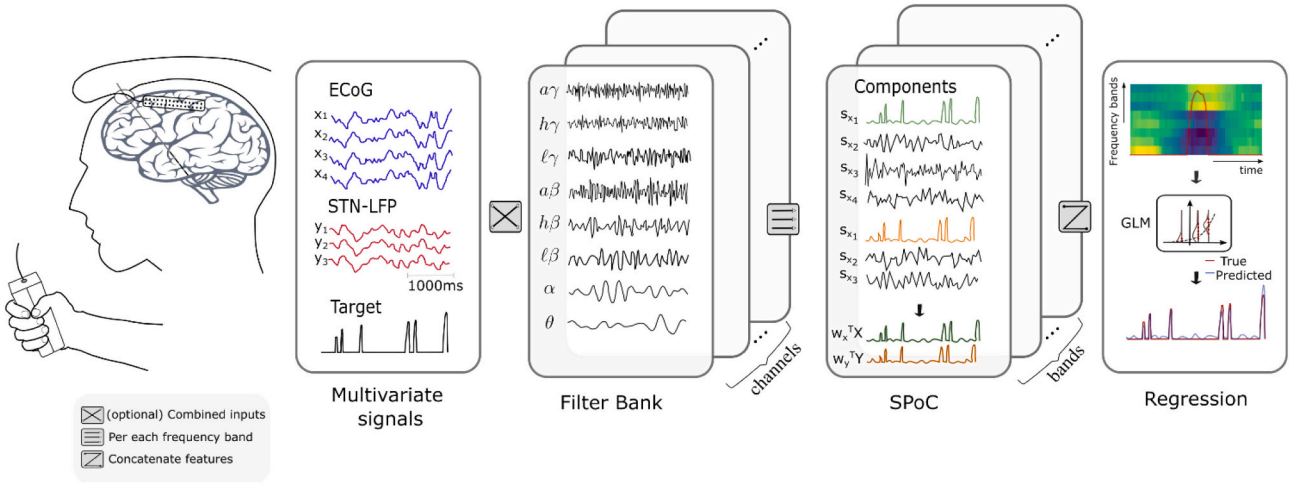

Fig. 2. Schematic representation of the decoding pipeline. Segments of 1000 ms from the invasive multi-channel recording were decomposed in eight frequency bands. The supervised spatial filtering SPoC method was applied at each frequency band, extracting the source more correlated to the hand grip movement (target variable). One spatio-spectral feature was extracted from each frequency band. Movement decoding was based on a GLM regression model, in which a Poisson sparse penalized regularization was implemented. Here θ: [4–8] Hz,α: [8–12] Hz, ℓβ: [13−20] Hz, hβ: [20–35] Hz, aβ:[13–35] Hz, ℓγ: [60–80] Hz, hγ: [90–200] Hz, and aγ: [60–200] Hz.

values equal to zero correspond to rest while values above zero correspond to the grip-force applied by the subject.

2.2. Spatio-spectral multiple recording site decoding pipeline

A subject-specific invasive neurophysiology movement decoding model that combines a filter-bank analysis with a spatial filtering approach was implemented. Data segments of 1000 ms were decomposed in eight frequency bands. Then the supervised SPoC spatial filtering approach was applied at each frequency band, extracting one spatio-spectral feature per frequency band considered. The resulting feature vector was used as input to a GLM with Poisson-like distribution sparse regression. A visual representation of the model is shown in Fig. 2. The decoding pipeline consists of three online-compatible main steps: i) data pre-processing, ii) feature learning and iii) movement decoding.

2.2.1. Online-compatible data pre-processing

Considering real-world applications, pre-processing steps should account for online real-time decoding challenges, that is, data is only available in packets, and future packets from the time point of decoding are not available to the decoder or processing pipeline. Thus, in this work, consecutive epochs of 1000 ms in step of 100 ms were extracted from the brain recording in order to continuously decode the grip-force target. All epochs were notch (60/120/180 Hz) and band-pass filtered by a 1000 ms FIR filter with a 4 Hz width transition band in eight frequency bands of interest θ: [4–8] Hz,α: [8–12] Hz, lowβ: [13–20] Hz, highβ: [20–35] Hz, allβ:[13–35] Hz, lowγ: [60–80] Hz, highγ: [90–200] Hz, and allγ: [60–200] Hz). Note that the frequency band from 35 to 60 Hz was not considered within this analysis to avoid the possible overlap between the desynchronization and resynchronization responses that may jointly appear at that band. In addition, we avoided working at a frequency range perturbated by the line noise.

The pre-processed brain recordings were arranged in a four-dimensional array accounting for the number of extracted epochs N_t, the number of channels N_c, the numbers of sample points per epoch N_s and the number of filter-bands N_f. In the case of the target variable, in accordance with the 1000 ms time window length extracted in steps of 100 ms, it was downsampled by selecting the 100th sample point from the processed grip-force. These online-compatible pre-processing steps were made by the py_neuromodulation package (https://github.com/neuromodulation/py_neuromodulation).

2.2.2. Feature extraction via source power comodulation

Electrophysiological recordings can be modeled as a linear and instantaneous superposition of neural sources (Baillet et al., 2001; Parra et al., 2005). Let $\mathbf{x}(t) \in \mathbb{R}^{N_c}$ be the brain recordings in the sensor space (raw data) at time t, where N_c denotes for the number of channels. Let $\boldsymbol{s}(t) \in \mathbb{R}^{N_c}$ be the sources (or components) and let $\boldsymbol{A} \in \mathbb{R}^{N_c \times N_c}$ be the mixing matrix, whose i^{th} column vector $\boldsymbol{a}_i$ is what is known as *spatial pattern*. Considering additive noise, the following definition holds to represent the generative model:

$$\boldsymbol{x}(t) = \boldsymbol{A}\boldsymbol{s}(t) \tag{1}$$

In the context of spatial filtering, the objective is to estimate $\boldsymbol{s}(t)$ and thus, transform the signal from the *sensor* to the *source* space. This sensor-to-source transformation can be obtained by means of source separation methods, as follows:

$$\widehat{\boldsymbol{s}}(t) = \boldsymbol{W}^T\boldsymbol{x}(t)$$

where $\boldsymbol{W} = [\boldsymbol{w}_1, \ldots, \boldsymbol{w}_i, \ldots, \boldsymbol{w}_{N_c}]$ is a $N_c \times N_c$ demixing matrix whose i^{th} column vector corresponds to what is known in the literature as *spatial filter*. Each of the spatial filter is meant to extract the signal from one source while suppressing the activity of the others, such that the resulting projected signal is a close approximation of the original source signal (Dähne et al., 2014). In the particular case of the SPoC algorithm, method simultaneously discovered by (Dähne et al., 2014; de Cheveigné and Parra, 2014), the information contained in the target variable is used to guide the decomposition. Denoting $\boldsymbol{z}(t)$ to the target variable (grip-force movement), the first SPoC filter is found by:

$$\boldsymbol{w}_{spoc} = \text{argmax}_{\boldsymbol{w} \in R^{N_c}} \frac{\boldsymbol{w}^T\boldsymbol{C}_z\boldsymbol{w}}{\boldsymbol{w}^T\overline{\boldsymbol{C}}\boldsymbol{w}},$$

where $\overline{\boldsymbol{C}} = \frac{1}{N_t}\sum_i^{N_t}\boldsymbol{C}_i$ is the Euclidean average covariance matrix across the N_t data segments and $\overline{\boldsymbol{C}_z} = \frac{1}{N_t}\sum_i^{N_t} z_i\boldsymbol{C}_i$ is the weighted average covariance matrix. The rest of the filters are obtained by solving a generalized eigenvalue decomposition problem (Dähne et al., 2014). As shown in (Sabbagh et al., 2020), the matrix $\boldsymbol{W}_{spoc}$ recovers the inverse of mixing matrix $\boldsymbol{A}$ defined in Eq. (1).

When data has been band-pass filtered, the power of the projected signal $\mathbf{w}^T\mathbf{x}(t)$ approximates the target function $\boldsymbol{z}(t)$. Thus, after applying SPoC spatio-spectral features can be extracted by $\text{var}[\boldsymbol{w}^T\boldsymbol{x}(t)]$.

In this work, the SPoC method was applied at each frequency band

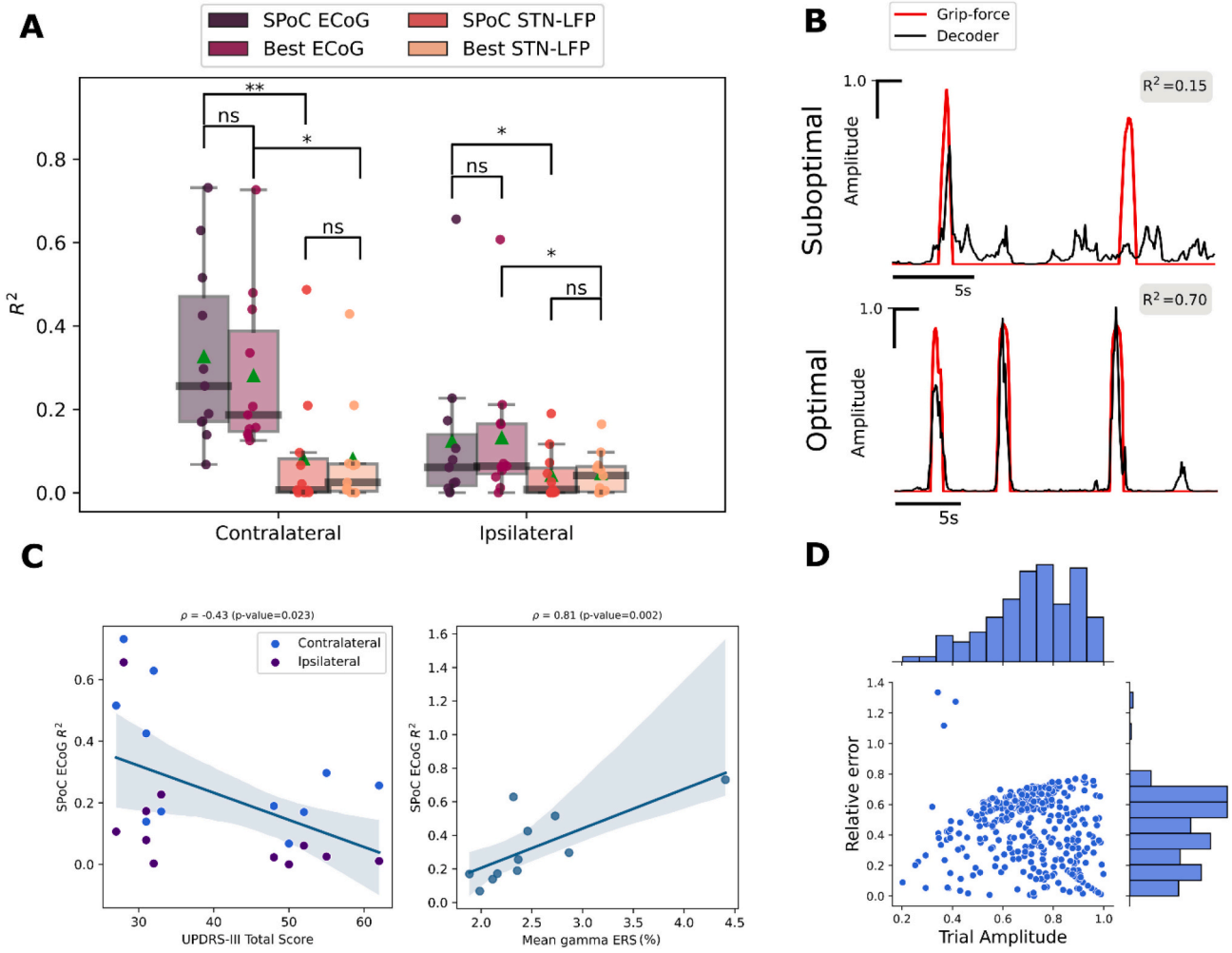

Fig. 3. Spatio-spectral brain signal decoding approaches can be applied in invasive neurophysiology. a) Performance comparison between the spatio-spectral approach (based on SPoC) and the single-channel (Best single recording location) approach, evaluated for each type of brain signal: ECoG and STN-LFP. The performance in decoding contralateral and ipsilateral movement is shown separately. Statistical significance according to Friedman + Nemenyi test is denoted by ** (p-value ≤ 0.01), * ($0.01 <$ p-value ≤ 0.05). The green triangle indicates the mean value, while individual subject's performance is represented as dots. b) Examples of true and decoded grip-force (normalized) for an optimal and a suboptimal case. c) SPoC ECoG patient decoding performance with respect to symptom severity and gamma ERS %. d) SPoc ECoG contralateral trial amplitude estimation error with respect to true trial amplitude. Here every dot represents a trial. (For interpretation of the references to colour in this figure legend, the reader is referred to the web version of this article.)

considered. Each band-power feature was extracted from the projected signal in the first SPoC component, taking the entirely 1000 ms for the θ band, last 500 ms for α, last 330 ms for the β bands and last 100 ms for the γ bands. Thus, at the end of the procedure eight (8) spatio-spectral features were computed. It is timely to mention here that while offline learning of the spatial filters $\boldsymbol{W}_{spoc}$ is needed, once such a matrix (or vector) is learned, the spatio-spectral features can be extracted in real-time by projecting the signals through $\boldsymbol{W}_{spoc}$.

2.2.3. Generalized regularized linear models

Let $\boldsymbol{H} \in R^{N_p \times N_t}$ be the matrix of N_p predictors (features), where N_t is the number of extracted epochs. Let $\boldsymbol{z} \in \mathbb{R}^{N_t}$ be as before, the target variable. Traditional linear model assumes that the distribution of the output is normal ($z \sim \mathcal{N}$) and thus, it can be modeled as a linear combination of the predictors and suitable weights, that is:

$$z = \beta_0 + \boldsymbol{\beta}\boldsymbol{H} + \boldsymbol{\epsilon}$$

where the model parameters $\beta_0, \boldsymbol{\beta} \in R^{N_p}$ can be estimated using ordinary least squares or its regularized versions. In the particular case of the elastic-net penalty (enet), a compromise between the l_1 and l_2 norm of the solution is imposed, and thus the solution vector and intercept can be found by solving the following unconstrained regularized problem:

$$\min_{\beta_0,\boldsymbol{\beta}} \frac{1}{N}\sum_{i=1}^{N} \mathscr{L}\left(z_i, \beta_0 + \boldsymbol{\beta}^T \mathbf{h}_i\right) + \lambda\left[\frac{1}{2}(1-\alpha)|\boldsymbol{\beta}|_2^2 + \alpha|\boldsymbol{\beta}|_1\right] \quad (2)$$

where $\mathscr{L}(\cdot)$ is the loss function aimed to be minimized, $\boldsymbol{h}_i$ is the i^{th} column vector of $\boldsymbol{H}$, and λ and α are positive constants called regularization parameters. In particular, $\alpha \in [0,1]$ and thus it balances between the Ridge regression ($\alpha = 0$) and LASSO regression ($\alpha = 1$).

When working with non-normally distributed outputs, we can extend this approach by means of generalized linear models (GLMs). The Poisson distribution is a discrete probability distribution that expresses the probability of a given number of events occurring in a fixed interval of time. Since the grip-force target is a non-negative output which accounts for rest and movement events, we assume here, from practical reasons, that $\boldsymbol{z}$ can be modeled as coming from a Poisson-like distribution. Under this assumption, a *log - exp* relationship between the predictors and the output exists. Using the softplus formulating proposed by (Dugas et al., 2001), the loss function $\mathscr{L}(\cdot)$ in Eq. (2) is given by:

$$\mathscr{L}(\beta_0, \boldsymbol{\beta}) = -\sum_i \{z_i log(\kappa_i) - \kappa_i\}, \quad \text{with} \quad \kappa_i = log\left(1 + exp\left(\beta_0 + \boldsymbol{\beta}^T \boldsymbol{h}_i\right)\right)$$

In the context of this study, each row of the matrix of predictor $\boldsymbol{H}$ is an 8-dimensional vector of spatio-spectral features extracted at each frequency-band via SPoC (see section 2.2.2 Feature extraction via source power comodulation).

2.2.4. Model training and evaluation

In order to investigate the practical use of the spatial filters for the development of aDBS, different computational experiments were conducted. Since the dataset comprised bilateral movements (contra- and ipsilateral to the electrodes' position on the respective hemisphere), one decoding model was built for each subject at each movement laterality. A 5-fold non-shuffled cross-validation procedure was performed, where the coefficient of determination R^2 was used for measuring the performance of the predicted grip-force when compared to the true grip-force output. The SPoC algorithm was applied as a feature extraction method at each frequency band considered. The demixing matrix $\boldsymbol{W}_{spoc}$ was learned using the training set in each cross-validation fold, and features from the unseen testing set were extracted using these estimated filters. For sake of comparison with the single electro approach, one spatial filter was used to compute the feature at each frequency band, leading to eight spatio-spectral features at the end of the filter-bank analysis. Features were concatenated and z-score scaled. In order to avoid any circularity, the statistics (mean and standard deviation) were estimated in the training set and then applied to scale the unseen testing test. These features corresponded to the inputs to the Poisson-like GLM with enet penalty regression model. In order to equally balance the Ridge and Lasso penalty, we set the α parameter of Eq. (2) equal to 0.5. The regularization parameter λ was searched via Bayesian Optimization (Snoek et al., 2012) over a 3-fold non-shuffled cross-validation on training data. Statistical analyses were performed via the non-parametric Friedman test and the post-hoc Nemenyi test at level of significance 0.05 (Demšar, 2006).

3. Results

3.1. Spatio-spectral features inform movement in PD patients

The SPoC method is designed to decompose, in a supervised manner, the multivariate brain recordings into a set of source components. In theory, if enough training data is available for building the decoding model, performance should be superior to that of a univariate approach. The advantages of using spatial approaches are well-known for surface EEG based decoding (Dähne et al., 2014), but given the more immediate relationship of sensor and source, the impact of spatial methods for invasive neurophysiology remains to be elucidated. Here, we compared the decoding capacity of our proposed spatio-spectral decoding model to a single channel pipeline (Merk et al., 2022). While the former uses all channels at once to build the model, the latter needs to evaluate the decoding capacity of each electrode individually and then choose the best electrode in training data to then run the movement prediction in testing data. For fair comparison purposes, for the single electrode approach, ECoG data were montaged with a common average reference before epoching. The comparative results are shown in Fig. 3A. Each dot, at each tested model, represent a participant-specific decoding performance calculated as the average across validation splits. The decoded and true grip-force for two patients (Optimal and Suboptimal case) are shown in Fig. 3B.

We first found that a decoding model based on contralateral movements performed better than its ipsilateral counterpart (e.g., mean R^2 SPoC ECoG contralateral: 0.32, mean R^2 SPoC ECoG ipsilateral: 0.13, p-value <0.01). Second, decoding based only on ECoG recording was consistently better than that based only on STN-LFP signals (e.g., mean R^2 SPoC ECoG contralateral: 0.32, mean R^2 SPoC STN-LFP contralateral: 0.08, p-value <0.01). Third, the spatial information seemed to have the potential to improve the decoding capacity of the model (e.g., mean R^2 SPoC ECoG contralateral: 0.32, mean R^2 Best ECoG contralateral: 0.28, p-value = 0.6), as indicated by the fact that two out of the three best decoding values came from patients' data with high-density ECoG electrode grid (28 contacts, 4 mm center to center).

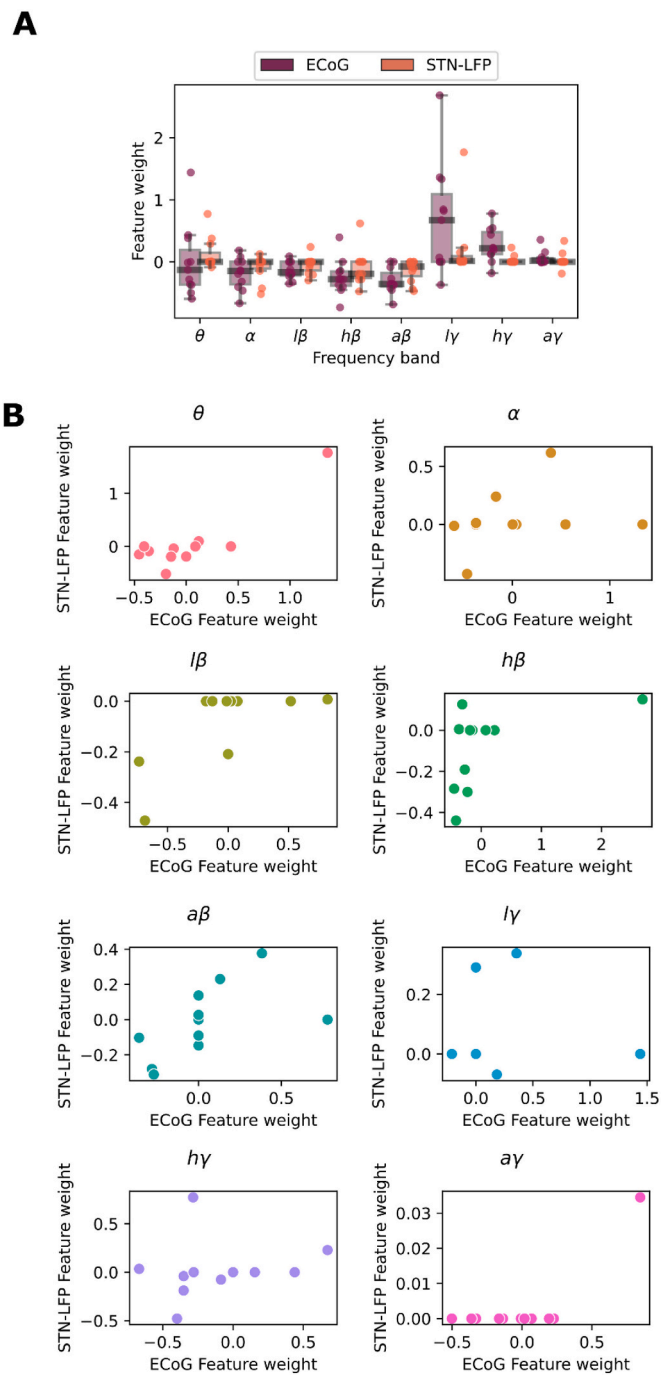

Fig. 4. Associated feature weights for cortical and subcortical data. a) Distribution of feature weights in cortical and subcortical data for contralateral movement grouped by frequency band. Weights equal to zero indicate that the regression model did not select such a feature for constructing the decoder. b) STN-LFP feature weights against ECoG feature weights for each frequency band. Here dots represent patients.

In order to understand performance variability across patients, correlation analyses were performed. First, the R^2 found by SPoC ECoG was correlated to patients' symptom severity measured by the UPDRS-III total score. Second, the percentage of event related synchronization (ERS %) in the low gamma band ([60–90] Hz) was calculated in 2.7 s epochs surrounding movement onset (0.7 s premovement and 2 s of

post-movement). Then, the mean ERS % across ECoG contacts was compared to the found R^2. As shown in Fig. 3C, a significant negative correlation exits between the decoding performance and symptom severity while a strong positive correlation was found between the amplitude of the ERS and decoding performance.

In addition, to understand if higher grip-force trial were harder to decode, the relative error between the true and estimated trial amplitude was jointly plotted against the true amplitude (Fig. 3D). As can be shown, there is no clear tendency between the applied grip-force and decoding performance.

3.1.1. Feature importance analysis from cortical and subcortical recordings

Spatio-spectral feature were extracted from 8 frequency bands and used as inputs to a GLM with sparse penalization (enet). Investigating the associated feature weights for the entire cohort for both cortical and subcortical data will give us insights about common feature importance across patients and between recording sites. The distribution of feature weights is shown in Fig. 4a for both ECoG and STN-LFP contralateral models, grouped by frequency band. Feature weights show the conditional dependence between the feature and the target variable (grip-force) when the other features remain constant. That is, a positive feature weight value indicates that an increment in such a frequency band contributes to grip-force decoding, while the opposite happens for negative feature weights. Since an enet penalization was imposed when constructing the model, a feature weight equal to zero indicates that such a frequency band was not utilized for building the movement decoder model. We can see that for the cortical model, in most of the cases all gamma band (aγ) is zeroed out, while high and low gamma present positive weights across the entire cohort. Negative feature weights are commonly assigned to low frequency bands, being the all beta and high beta bands the most selected. STN features weights varied in a lower range as compared to ECoG. Interesting, and particularly for subcortical data, low frequency bands seem to be more informative for constructing the decoding model than high frequency features. When analyzing the one-to-one correspondence between cortical and subcortical feature weights we see that subcortical models seem to rely more on low-frequency bands (Fig. 4b).

3.2. Combining cortical and subcortical spatio-spectral features does not improve movement decoding

ECoG and STN-LFP signals were recorded simultaneously in these participants, allowing the definition of decoding models trained on a combination of both recording site signals. The spatio-spectral features were extracted from 8 frequency bands, resulting in overall 16 input features (8 features per modality). Fig. 4 shows the performance of the decoding model using ECoG + STN-LFP recordings against decoding models that only use either ECoG or STN data. The statistical analysis indicates that there are no significant differences between the combined ECoG + STN-LFP decoding model and the decoding model based only on ECoG signals (p-value = 0.9).

3.2.1. Model interpretability

Although on average combining spatio-spectral features from cortical and subcortical recording did not outperform the approach using only ECoG, we further analyzed those cases in which the combinational use did improve movement decoding. Thus, for three patients in which performance improvement was found by adding the STN signal to the ECoG decoding model, a detailed model interpretability analysis was performed.

Fig. 6 shows the feature weights from the GLM constructed based upon using ECoG + STN-LFP features together with the learned spatial patterns from the cortical and subcortical signals at each frequency band considered. As before, a positive feature weight value at a given frequency band indicates that an increment in such a frequency band positive contributes to grip-force decoding, when the other features remain constant. Interestingly, for these subjects, the decoding model depends on spatio-spectral features coming from both cortical and subcortical regions, being the former still more informative for the decoding. The spatial patterns from selected features map movement-related brain activity.

4. Discussion

In this study we implemented a spatio-spectral approach to decode movement using invasive brain recordings in patients with Parkinson's disease. The supervised spatial filter SPoC method was used to extract features at eight pre-defined frequency bands. The predictive model was built via GLM with regularized Poisson-like sparse regression. Contra- and ipsilateral movements were decoded separately. First, the spatio-spectral approach was compared against a single channel approach. Second, the decoding pipeline was tested using combined ECoG and subthalamic LFP recordings and compared to models only informed by ECoG. Model interpretability was assessed by analyzing model feature weights and cortical and subcortical source maps.

Spatial information in invasive neurophysiology. The use of source separation methods has been largely investigated for understanding brain networks by using different brain imaging modalities. These methods have one objective in common: recovering the unknown (unobservable) source signals that explain the observable brain activity (Silva et al., 2016). The statistical generative models on which the spatial filtering methods rely on, assume that the recorded brain activity is a consequence of the distributions of different rhythms across electrode contacts (see Fig. 1).

In invasive neurophysiology, as compared to non-invasive electro- or magnetoencephalography, the recordings have a better spatial accuracy, yet there is still a considerable overlap between the activity of different sources at a given electrode (Volkova et al., 2019). In this work, we used a supervised spatial filtering approach for finding the neural source more correlated in power to the movement task. The performance of this spatial filtering method was compared against a similar decoding model which relies on correlating the power of a single recording location with movement (Merk et al., 2022). Our results showed that introducing the spatial information to a band-power decoding model has the potential to improve decoding capacity in invasive neurophysiology (see Fig. 3). In particular, this improvement was observed for the ECoG recording but not for the STN-LFP. This could be explained by the fact that in our cohort the STN-LFP were recorded by using 4 contacts separated by 0.5 mm (see subsection 2.1 Data, in Materials and Method), and thus minimal relative spatial information could be extracted. Similarly, most of the ECoG recordings were acquired by using low-dimensional ECoG grids (6 or 8 contacts). Based on the fact that two out of the three best ECoG contralateral movement decoding came from those patients with largest electrode grid (28 contacts), we argue that higher improvement could potentially be found for larger high-density ECoG electrodes.

Bipolar montage can be viewed as the application of a particularly simple spatial filter which aim to extract locally generated signals (Schaworonkow and Voytek, 2021). Here, LFP from the STN were bipolarly re-referenced before running the decoder. While such a preprocessing step reduces the rank of the signal and transform it into a new sensor space, which could reduce the spatio-spectral feature extraction power, for emulating clinical setups, bipolar re-referencing should still be applied as a preprocessing step for STN-LFP. Since the referencing choice highly impacts the source dynamic of the resulting signal, there is no doubt that further research is needed to understand the impact and necessity of traditional re-referecing steps before feature learning for clinical adaptive DBS settings.

One of the biggest advantages of using data-driven spatial filtering approaches for feature learning is that the information captured by any given number of electrodes contacts can be collapse on a lower dimensional space. Extracted features are then calculated from a linear combination across electrodes contacts, which in the case of SPoC, band

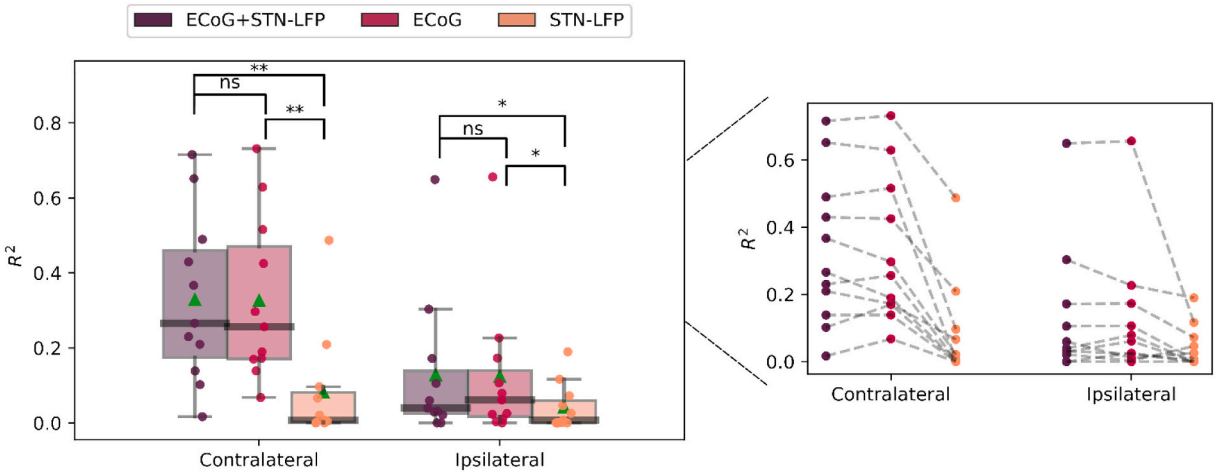

Fig. 5. Adding STN-LFPs features does not significantly improve ECoG-based decoding. Performance comparison between multiple recording sites and single recording site approaches. The performance in decoding contralateral and ipsilateral movements is shown separately. The green triangle indicates the mean value, while individual subject's performance is represented as dots. The plot on the right links decoding performance across the same subject (dot) when using STN, ECoG and ECoG + STN-LFP data. Statistical significance according to Friedman + Nemenyi test is denoted by ** (p-value $\leq$ 0.01), * (0.01 $<$ p-value $\leq$ 0.05). (For interpretation of the references to colour in this figure legend, the reader is referred to the web version of this article.)

power feature learning goes beyond merely taking the average band power across electrodes. In that sense, the relevance of electrode location is mostly based on the broad coverage of target areas rather than local specific targets.

Low frequency oscillations are more informative for movement decoding. Model feature weights inspection showed that spatio-spectral features extracted from low frequency oscillations are more informative for movement decoding than those extracted from the high frequency bands. In fact, for subcortical recordings, low frequency extracted features were the main source of discriminative information. This strong bias towards low frequency bands features can be explained by the fact that our data only includes medication off patients, and thus a prominent beta activity is likely to occur (López-Azcárate et al., 2010). The suppression in beta activity due to for example levodopa treatment, can debias the decoder to rely on features beyond the beta band. Interesting, for ECoG signal higher features values, in the absolute value sense, were found for low gamma frequency band, indicating that the most relevant spatio-spectral information for force decoding from the cortex is driven by beta and low gamma bands. Studies on STN recordings have already shown that gripping force is mostly encoded in the beta (13–30 Hz) and low gamma (55–90 Hz) bands (Shah et al., 2018; Tan et al., 2016).

Combining spatio-spectral features from multiple site recordings. Several works have investigated the relationship between STN oscillations and those from cerebral cortex in patients with PD. It has been shown that the beta band of the STN is coupled with the cortex activity in PD patients, and that such coupling changes with medication level (Williams et al., 2002). Recently, the phase-locking between STN oscillations and cortical beta oscillations has been reported to be different with respect to the cortical areas being studied (Sharott et al., 2018). Thus, we investigated how the combinational use of spatio-spectral features coming from simultaneously recorded cortical and subcortical activity could impact decoding performance. On average, we found no gain when adding the STN-LFP features to the ECoG approach with respect to using only ECoG features. The fact that no improvement was found in the combinational use of STN-LFP and ECoG features, however, could reflect the fact that we explored here only features that rely on the band power information of the brain oscillations. In fact, recently coherence between STN and motor cortex was shown to be relevant for differentiating motor states in PD patients (Gilron et al., 2021).

Interestingly, there were cases in which the combination of ECoG and LFP recordings approach did improve the decoding capacity when compared to models informed by ECoG alone. To understand the underlying mechanisms that led to such improvement, the decoding model for those particular subjects was analyzed. One of the main advantages of using linear matrix-based separation methods for finding the neural sources is that the solution is neurophysiologically interpretable. Since also a linear model was used to learn the mapping between features and movement target output, the coefficient values of the solution can also be interpreted to understand feature importance. Fig. 6 shows, for three subjects, the solution coefficient values (feature weights) associated to each spatio-spectral feature across the different brain modalities and frequency bands. Common to these subjects is that both ECoG and STN coefficients show a strong spatial pattern, with a frequency specific spatial peak of feature importance. Moreover, we note although ECoG features have the largest coefficient values, low frequency STN-LFP features are also selected. This behavior, despite the fact that features were stacked to conform a unique input vector to the GLM, presents a similar feature weights association at when two decoding models were fitted separately from cortical and a subcortical data.

When analyzing the spatial maps, we observed that the shape of the spatial patterns differs across subjects and frequency bands. Here, high-frequency oscillations have limited spatial spread (the component contributes to recordings from few electrodes, and thus abrupt changes are observed in the spatial patterns) while low-frequency oscillations present higher spatial spread, meaning that the source is contributing to recordings from several electrodes (Muller et al., 2016; Schaworonkow and Voytek, 2021). The individual spatial information cannot be inferred a priori, but by visual inspecting the spatial patterns, feature importance, and model decoding could be anticipated.

We would like also to note here the superiority of ECoG over STN-LFP for movement decoding (see Figs. 3 and 5). These findings are in line with Merk et al. (Merk et al., 2022) and could be explained by the fact that ECoG recordings have a better spatial coverage (more electrode contacts), providing a much stronger signal and allowing measurements of higher amplitude oscillations than depth recordings (Panov et al., 2017).

The importance of individualized subject specific decoding models. For clinical standardization and out-of-the-box use of machine learning powered brain computer interfaces in the future, the development of cross-patient decoding approaches would be beneficial. However, the results of our study highlight the importance of subject-dependent decoding models. Across patient variability is explained by the severity of motor symptoms (Fig. 3C), which has been observed in

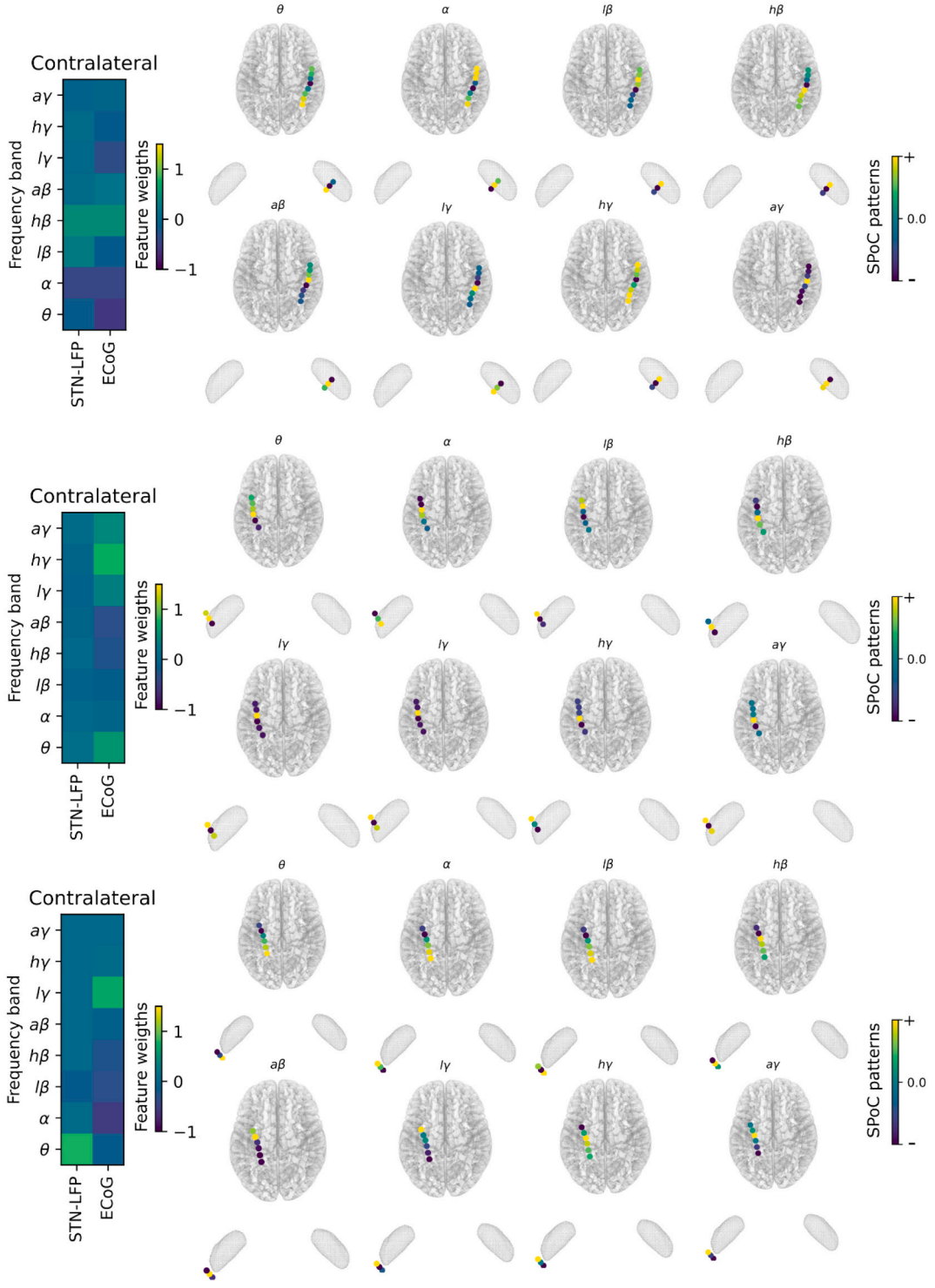

Fig. 6. Spatio-spectral information shows feature importance and maps brain activity related to grip-force encoding. Model interpretability for three subjects in which the multisite recording site outperforms the single site ECoG decoding capacity. One subject per figure subpanel. Left side: GLM coefficient values (feature weights); right side: the associated spatial pattern at each frequency band considered. Due to the nature of the Poisson-like distribution, for better interpretation of the output, the coefficient values were transformed by taking the exponential and subtracting a unit.

different movements associated with a reduction in beta but an increment in gamma band activity (Tan et al., 2019). Here we have also shown that cortex low gamma ERS can predict cortical grip-force decoding.

When analyzing the spatio-spectral patterns difference exist between patients, which could make such an across-patient implementation difficult. Since spatial filters were used to extract the band-power features, we could investigate the neural activity at each electrode location in each frequency band, by plotting the corresponding spatial pattern (Fig. 6). The spatial pattern at each frequency band reflects the mapping (in strength and sign) of the movement task-related source at each electrode. Although some brain maps across subjects share similarities, each subject has its own spatial map at each frequency band. Ultimately, for clinical brain computer interfaces, the individual spatio-

spectral activity patterns will be more informative for a patient specific precision medicine approach to adaptive deep brain stimulation.

Limitations. Several limitations of this study are worth noting. First, we based our analyses on data obtained with a grip-force task, which describes just one type of motor behavior. Second, the data was recorded during DBS implantation surgery, when participants were without medication or neurostimulation, which represents only one possible PD condition. Given that such conditions change the state of recorded brain activity, further research is needed to account for these potential sources of variability. Thirdly, the number of patients and number of trials perform by each patient was low. While the former restrings the decoding capacity of the model, the latter limits detailed analysis of result interpretability. In addition, the number of contacts in both STN and cortex recordings was sometimes too low to appreciate the spatial information of the signals. Lastly, our numerical experiments were based on a single session per patient. Considering the lack of stationarity in the electrophysiological brain data, future models ideally should be tested in several recording sessions, acquired at different days.

Clinical relevance. While grip-force decoding per se, may not be required for adaptive stimulation paradigm, we would like to argue that it is a very good application to investigate decoding methods, because it allows a fine-grained analysis of brain signals and behavior. Importantly, grip-force represents movement vigor, which is known to be modulated by the basal ganglia and the STN (Lofredi et al., 2018) and can be impaired in PD. Independent of the specific target variable of grip-force, the results shown here are likely transferrable to other domains of symptom and behavior decoding, which may be augmented by spatio-spectral methods in specific patients. That is the case of aDBS for essential tremor (ET), in which authors have shown that adaptive algorithms can be constructed based on extracted features from the thalamus (He et al., 2020) or the cortex (Herron et al., 2017). We argue that the incorporation to spatio-spectral features for the development of intelligence algorithm would benefit ET treated by DBS.

In this study we have shown that decoding movement from spatio-spectral features extracted from cortical oscillations has the potential to improve decoding performance as compared to basal ganglia signals. However, decoding from STN-LFP signals have been largely study in the community, most probability due to fact that brain monitoring can be done on a basic of a unique implantation site, without the need of additional electrodes or hardware (Little and Brown, 2012). Changes in the beta band of STF-LFP signals have already been studied as a putative biomarker for bradykinesia prediction (Kehnemouyi et al., 2022) but similar studies based on ECoG recordings are still missing. Accounting for multichannel approaches that ultimately yield comparative movement decoding performances as single electrode decoding frameworks, potentially introduces more flexibility in the design of intelligence adaptive DBS devices. The localization of the detector(s) contact(s) will impact less in the decoding capacity since distributed patterns across electrodes are extracted with spatial filtering methods. In addition to this, it has the potential to integrate neural recordings from different but additional brain areas of the sensorimotor network, which is expected to improve BCI decoding (Gallego et al., 2022).

In conclusion, we have shown that movement decoding could benefit from i) the use of the spatial information and ii) multimodal brain recordings. Our results suggest that by combining two recording modalities both the decoding capacity of the model and model robustness can be improved in some cases, but an individual assessment of features and model performances is required to achieve optimal decoding performances. The high impact contribution of cortical recording for movement decoding supports the utility of ECoG for future invasive bidirectional BCI devices.

Data and code availability

The corresponding Python source codes developed for this work are publicly available at https://github.com/Brain-Modulation-Lab/Paper_SpatialPatternsMovementDecoding. We used the py_neuromodulation package (https://github.com/neuromodulation/py_neuromodulation) for implementing the online-compatible pre-processing steps, the MNE-Python library(Gramfort et al., 2013) (https://mne.tools) for implementing SPoC, the pyglmnet package (https://pypi.org/project/pyglmnet/) for running the GLM (Jas et al., 2020), scikit-learn for constructing pipelines (Pedregosa et al., 2011) (https://scikit-learn.org), and the Bayesian Optimization package (https://github.com/fmfn/BayesianOptimization) for finding the optimal regularization parameter.

The data that support the findings of this study are available upon reasonable request. A formal data sharing agreement is required.

CRediT authorship contribution statement

Victoria Peterson: Conceptualization, Methodology, Software, Validation, Formal analysis, Writing – original draft, Visualization. **Timon Merk:** Software, Data curation, Writing – review & editing. **Alan Bush:** Conceptualization, Investigation, Data curation, Writing – review & editing. **Vadim Nikulin:** Conceptualization, Methodology, Writing – review & editing. **Andrea A. Kühn:** Conceptualization, Writing – review & editing, Project administration, Funding acquisition. **Wolf-Julian Neumann:** Conceptualization, Writing – review & editing, Supervision, Project administration, Funding acquisition. **R. Mark Richardson:** Conceptualization, Investigation, Writing – review & editing, Supervision, Project administration, Funding acquisition.

Declaration of Competing Interest

The authors declare no conflict of interest. The funders had no role in the design of the study; in the collection, analyses, or interpretation of data; in the writing of the manuscript, or in the decision to publish the results.

Data availability

The data that support the findings of this study are available upon reasonable request. A formal data sharing agreement is required. Code is available at GitHub, as indicated in the manuscript.

Acknowledgments

We would like to thank the subjects for their generous gift of time in the operating room and additional experimenters who acquired and organized the data. In addition, we would like to thank Denis A. Engemann for suggesting the use of a generalized linear model with non-negative distributions. The present manuscript was supported through a US-German Collaborative Research in Computational Neuroscience (CRCNS) grant, funded by the Federal Ministry for Research and Education (Germany) and the National Institutes of Health (United States, R01NS110424). In addition, this manuscript was partially funded by the Deutsche Forschungsgemeinschaft (DFG, German Research Foundation) – Project-ID 424778381 – TRR 295.

References

Alhourani, A., Korzeniewska, A., Wozny, T.A., Lipski, W.J., Kondylis, E.D., Ghuman, A.S., Crone, N.E., Crammond, D.J., Turner, R.S., Richardson, R.M., 2020. Subthalamic nucleus activity influences sensory and motor cortex during force transduction. Cereb. Cortex 30, 2615–2626. https://doi.org/10.1093/cercor/bhz264.

Baillet, S., Mosher, J.C., Leahy, R.M., 2001. Electromagnetic brain mapping. IEEE Signal Process. Mag. 18, 14–30. https://doi.org/10.1109/79.962275.

Cagnan, H., Denison, T., McIntyre, C., Brown, P., 2019. Emerging technologies for improved deep brain stimulation. Nat. Biotechnol. 37, 1024–1033. https://doi.org/10.1038/s41587-019-0244-6.

Castaño-Candamil, S., Piroth, T., Reinacher, P., Sajonz, B., Coenen, V.A., Tangermann, M., 2020. Identifying controllable cortical neural markers with machine learning for adaptive deep brain stimulation in Parkinson's disease. Neuroimage Clin. 28, 102376 https://doi.org/10.1016/j.nicl.2020.102376.

de Cheveigné, A., Parra, L.C., 2014. Joint decorrelation, a versatile tool for multichannel data analysis. Neuroimage 98, 487–505. https://doi.org/10.1016/j.neuroimage.2014.05.068.

Dähne, S., Meinecke, F.C., Haufe, S., Höhne, J., Tangermann, M., Müller, K.R., Nikulin, V., 2014. SPoC: a novel framework for relating the amplitude of neuronal oscillations to behaviorally relevant parameters. Neuroimage 86, 111–122. https://doi.org/10.1016/j.neuroimage.2013.07.079.

Demšar, J., 2006. Statistical comparisons of classifiers over multiple data sets. J. Mach. Learn. Res. 7, 1–30.

Deuschl, G., Schade-Brittinger, C., Krack, P., Volkmann, J., Schäfer, H., Bötzel, K., Daniels, C., Deutschländer, A., Dillmann, U., Eisner, W., Gruber, D., Hamel, W., Herzog, J., Hilker, R., Klebe, S., Kloß, M., Koy, J., Krause, M., Kupsch, A., Lorenz, D., Lorenzl, S., Mehdorn, H.M., Moringlane, J.R., Oertel, W., Pinsker, M.O., Reichmann, H., Reuß, A., Schneider, G.H., Schnitzler, A., Steude, U., Sturm, V., Timmermann, L., Tronnier, V., Trottenberg, T., Wojtecki, L., Wolf, E., Poewe, W., Voges, J., 2006. A randomized trial of deep-brain stimulation for Parkinson's disease. N. Engl. J. Med. https://doi.org/10.1056/NEJMoa060281.

Dugas, C., Bengio, Y., Bélisle, F., Nadeau, C., Garcia, R., 2001. Incorporating second-order functional knowledge for better option pricing. Adv. Neural Inf. Proces. Syst. 472–478.

Feldmann, L.K., Neumann, W., Krause, P., Lofredi, R., Schneider, G., Kühn, A.A., 2021. Subthalamic beta band suppression reflects effective neuromodulation in chronic recordings. Eur. J. Neurol. ene.14801 https://doi.org/10.1111/ene.14801.

Ferleger, B.I., Houston, B., Thompson, M.C., Cooper, S.S., Sonnet, K.S., Ko, A.L., Herron, J.A., Chizeck, H.J., 2020. Fully implanted adaptive deep brain stimulation in freely moving essential tremor patients. medRxiv 2020.05.28.20092148. https://doi.org/10.1101/2020.05.28.20092148.

Gallego, J.A., Makin, T.R., McDougle, S.D., 2022. Going beyond primary motor cortex to improve brain-computer interfaces. Trends Neurosci. https://doi.org/10.1016/j.tins.2021.12.006.

Gilron, R., Little, S., Perrone, R., Wilt, R., de Hemptinne, C., Yaroshinsky, M.S., Racine, C. A., Wang, S.S., Ostrem, J.L., Larson, P.S., Wang, D.D., Galifianakis, N.B., Bledsoe, I. O., San Luciano, M., Dawes, H.E., Worrell, G.A., Kremen, V., Borton, D.A., Denison, T., Starr, P.A., 2021. Long-term wireless streaming of neural recordings for circuit discovery and adaptive stimulation in individuals with Parkinson's disease. Nat. Biotechnol. https://doi.org/10.1038/s41587-021-00897-5.

Gramfort, A., Luessi, M., Larson, E., Engemann, D.A., Strohmeier, D., Brodbeck, C., Goj, R., Jas, M., Brooks, T., Parkkonen, L., Hämäläinen, M., 2013. MEG and EEG data analysis with MNE-Python. Front. Neurosci. https://doi.org/10.3389/fnins.2013.00267.

He, S., Debarros, J., Khawaldeh, S., Pogosyan, A., Mostofi, A., Baig, F., Pereira, E., Brown, P., Tan, H., 2020. Closed-loop DBS triggered by real-time movement and tremor decoding based on thalamic LFPs for essential tremor, 44, pp. 3602–3605.

Herron, J.A., Thompson, M.C., Brown, T., Chizeck, H.J., Ojemann, J.G., Ko, A.L., 2017. Cortical brain–computer interface for closed-loop deep brain stimulation. IEEE Trans. Neural Syst. Rehabil. Eng. 25, 2180–2187. https://doi.org/10.1109/TNSRE.2017.2705661.

Jas, M., Achakulvisut, T., Idrizović, A., Acuna, D., Antalek, M., Marques, V., Odland, T., Garg, R.P., Agrawal, M., Umegaki, Y., 2020. Pyglmnet: Python implementation of elastic-net regularized generalized linear models. J. Open Source Softw. 5.

Kehnemouyi, Y.M., Wilkins, K.B., Anidi, C.M., Anderson, R.W., Afzal, M.F., Bronte-Stewart, H.M., Bronte-Stewart, H., Cahill, J.E., 2022. Modulation of beta bursts in subthalamic sensorimotor circuits predicts improvement in bradykinesia. https://doi.org/10.1093/brain/awaa463.

Kondylis, E.D., Randazzo, M.J., Alhourani, A., Lipski, W.J., Wozny, T.A., Pandya, Y., Ghuman, A.S., Turner, R.S., Crammond, D.J., Richardson, R.M., 2016. Movement-related dynamics of cortical oscillations in Parkinson's disease and essential tremor. Brain 139, 2211–2223. https://doi.org/10.1093/brain/aww144.

Little, S., Brown, P., 2012. What brain signals are suitable for feedback control of deep brain stimulation in Parkinson's disease? Ann. N. Y. Acad. Sci. 1265, 9–24. https://doi.org/10.1111/j.1749-6632.2012.06650.x.

Little, S., Pogosyan, A., Neal, S., Zavala, B., Zrinzo, L., Hariz, M., Foltynie, T., Limousin, P., Ashkan, K., FitzGerald, J., Green, A.L., Aziz, T.Z., Brown, P., 2013. Adaptive deep brain stimulation in advanced Parkinson disease. Ann. Neurol. 74, 449–457. https://doi.org/10.1002/ana.23951.

Lofredi, R., Neumann, W.-J., Bock, A., Horn, A., Huebl, J., Siegert, S., Schneider, G.-H., Krauss, J.K., Kuühn, A.A., 2018. Dopamine-dependent scaling of subthalamic gamma bursts with movement velocity in patients with Parkinson's disease. Elife 7. https://doi.org/10.7554/eLife.31895.

López-Azcárate, J., Tainta, M., Rodríguez-Oroz, M.C., Valencia, M., González, R., Guridi, J., Iriarte, J., Obeso, J.A., Artieda, J., Alegre, M., 2010. Neurobiology of Disease Coupling between Beta and High-Frequency Activity in the Human Subthalamic Nucleus May Be a Pathophysiological Mechanism in Parkinson's Disease. https://doi.org/10.1523/JNEUROSCI.5459-09.2010.

Merk, T., Peterson, V., Lipski, W.J., Blankertz, B., Turner, R.S., Li, N., Horn, A., Richardson, R.M., Neumann, W.-J., 2022. Electrocorticography is superior to subthalamic local field potentials for movement decoding in Parkinson's disease. Elife 11, e75126. https://doi.org/10.7554/eLife.75126.

Muller, L., Hamilton, L.S., Edwards, E., Bouchard, K.E., Chang, E.F., 2016. Spatial resolution dependence on spectral frequency in human speech cortex electrocorticography. J. Neural Eng. 13, 56013.

Neumann, W.J., Turner, R.S., Blankertz, B., Mitchell, T., Kühn, A.A., Richardson, R.M., 2019. Toward electrophysiology-based intelligent adaptive deep brain stimulation for movement disorders. Neurotherapeutics 16, 105–118. https://doi.org/10.1007/s13311-018-00705-0.

Opri, E., Cernera, S., Molina, R., Eisinger, R.S., Cagle, J.N., Almeida, L., Denison, T., Okun, M.S., Foote, K.D., Gunduz, A., 2020. Chronic embedded cortico-thalamic closed-loop deep brain stimulation for the treatment of essential tremor. Sci. Transl. Med. 12 https://doi.org/10.1126/scitranslmed.aay7680.

Panov, F., Levin, E., de Hemptinne, C., Swann, N.C., Qasim, S., Miocinovic, S., Ostrem, J. L., Starr, P.A., 2017. Intraoperative electrocorticography for physiological research in movement disorders: principles and experience in 200 cases. J. Neurosurg. 126, 122–131.

Parra, L.C., Spence, C.D., Gerson, A.D., Sajda, P., 2005. Recipes for the linear analysis of EEG. Neuroimage 28, 326–341. https://doi.org/10.1016/j.neuroimage.2005.05.032.

Pedregosa, F., Varoquaux, G., Gramfort, A., Michel, V., Thirion, B., Grisel, O., Blondel, M., Prettenhofer, P., Weiss, R., Dubourg, V., Vanderplas, J., Passos, A., Cournapeau, D., Brucher, M., Perrot, M., Duchesnay, É., 2011. Scikit-learn: machine learning in Python. J. Mach. Learn. Res. 12, 2825–2830.

Priori, A., Foffani, G., Rossi, L., Marceglia, S., 2013. Adaptive deep brain stimulation (aDBS) controlled by local field potential oscillations. Exp. Neurol. 245, 77–86. https://doi.org/10.1016/j.expneurol.2012.09.013.

Sabbagh, D., Ablin, P., Varoquaux, G., Gramfort, A., Engemann, D.A., 2020. Predictive regression modeling with MEG/EEG: from source power to signals and cognitive states. Neuroimage 116893. https://doi.org/10.1016/j.neuroimage.2020.116893.

Schaworonkow, N., Voytek, B., 2021. Enhancing oscillations in intracranial electrophysiological recordings with data-driven spatial filters. PLoS Comput. Biol. 17, 1–29. https://doi.org/10.1371/journal.pcbi.1009298.

Schuepbach, W.M.M., Rau, J., Knudsen, K., Volkmann, J., Krack, P., Timmermann, L., Hälbig, T.D., Hesekamp, H., Navarro, S.M., Meier, N., Falk, D., Mehdorn, M., Paschen, S., Maarouf, M., Barbe, M.T., Fink, G.R., Kupsch, A., Gruber, D., Schneider, G.-H., Seigneuret, E., Kistner, A., Chaynes, P., Ory-Magne, F., Brefel Courbon, C., Vesper, J., Schnitzler, A., Wojtecki, L., Houeto, J.-L., Bataille, B., Maltête, D., Damier, P., Raoul, S., Sixel-Doering, F., Hellwig, D., Gharabaghi, A., Krüger, R., Pinsker, M.O., Amtage, F., Régis, J.-M., Witjas, T., Thobois, S., Mertens, P., Kloss, M., Hartmann, A., Oertel, W.H., Post, B., Speelman, H., Agid, Y., Schade-Brittinger, C., Deuschl, G., 2013. Neurostimulation for Parkinson's disease with early motor complications. N. Engl. J. Med. 368, 610–622. https://doi.org/10.1056/NEJMoa1205158.

Shah, S.A., Tan, H., Tinkhauser, G., Brown, P., 2018. Towards real-time, continuous decoding of gripping force from deep brain local field potentials. IEEE Trans. Neural Syst. Rehabil. Eng. 26, 1460–1468. https://doi.org/10.1109/TNSRE.2018.2837500.

Sharott, A., Gulberti, A., Hamel, W., Köppen, J.A., Münchau, A., Buhmann, C., Pötter-Nerger, M., Westphal, M., Gerloff, C., Moll, C.K.E., Engel, A.K., 2018. Spatio-temporal dynamics of cortical drive to human subthalamic nucleus neurons in Parkinson's disease. Neurobiol. Dis. 112, 49–62. https://doi.org/10.1016/j.nbd.2018.01.001.

Silva, R.F., Plis, S.M., Sui, J., Pattichis, M.S., Adali, T., Calhoun, V.D., 2016. Blind source separation for unimodal and multimodal brain networks: a unifying framework for subspace modeling. IEEE J. Sel. Top. Signal Process. 10, 1134–1149. https://doi.org/10.1109/JSTSP.2016.2594945.

Sisterson, N.D., Carlson, A.A., Rutishauser, U., Mamelak, A.N., Flagg, M., Pouratian, N., Salimpour, Y., Anderson, W.S., Richardson, R.M., 2021. Electrocorticography during deep brain stimulation surgery: safety experience from 4 centers within the National Institute of Neurological Disorders and Stroke research opportunities in human consortium. Neurosurgery 88, E420–E426. https://doi.org/10.1093/neuros/nyaa592.

Snoek, J., Larochelle, H., Adams, R.P., 2012. Practical bayesian optimization of machine learning algorithms. Adv. Neural Inf. Proces. Syst. 25.

Swann, N.C., de Hemptinne, C., Thompson, M.C., Miocinovic, S., Miller, A.M., Gilron, R., Ostrem, J.L., Chizeck, H.J., Starr, P.A., 2018. Adaptive deep brain stimulation for Parkinson's disease using motor cortex sensing. J. Neural Eng. https://doi.org/10.1088/1741-2552/aabc9b.

Tan, H., Pogosyan, A., Ashkan, K., Green, A.L., Aziz, T., Foltynie, T., Limousin, P., Zrinzo, L., Hariz, M., Brown, P., 2016. Decoding gripping force based on local field potentials recorded from subthalamic nucleus in humans. https://doi.org/10.7554/eLife.19089.001.

Tan, H., Debarros, J., He, S., Pogosyan, A., Aziz, T.Z., Huang, Y., Wang, S., Timmermann, L., Visser-Vandewalle, V., Pedrosa, D.J., Green, A.L., Brown, P., 2019. Decoding voluntary movements and postural tremor based on thalamic LFPs as a basis for closed-loop stimulation for essential tremor. Brain Stimul. 12, 858–867. https://doi.org/10.1016/j.brs.2019.02.011.

Volkova, K., Lebedev, M.A., Kaplan, A., Ossadtchi, A., 2019. Decoding movement from electrocorticographic activity: a review. Front. Neuroinform. 13, 1–20. https://doi.org/10.3389/fninf.2019.00074.

Williams, D., Tijssen, M., van Bruggen, G., Bosch, A., Insola, A., Lazzaro, V., Mazzone, P., Oliviero, A., Quartarone, A., Speelman, H., Brown, P., 2002. Dopamine-dependent changes in the functional connectivity between basal ganglia and cerebral cortex in humans. Brain 125, 1558–1569. https://doi.org/10.1093/brain/awf156.

Wu, D., King, J.-T., Chuang, C.-H., Lin, C.-T., Jung, T.-P., 2018. Spatial filtering for EEG-based regression problems in brain–computer interface (BCI). IEEE Trans. Fuzzy Syst. 26, 771–781. https://doi.org/10.1109/TFUZZ.2017.2688423.

Xie, Z., Schwartz, O., Prasad, A., 2018. Decoding of finger trajectory from ECoG using deep learning. J. Neural Eng. 15 https://doi.org/10.1088/1741-2552/aa9dbe.